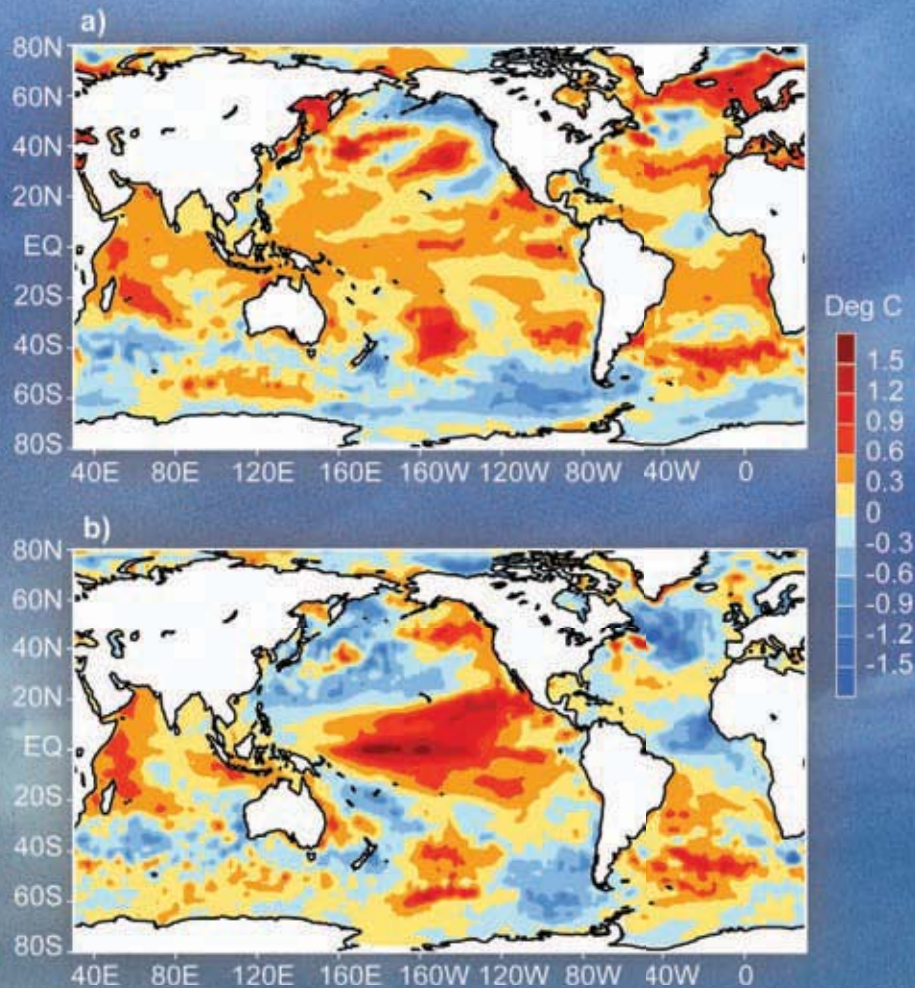


STATE OF THE CLIMATE IN 2009

D.S.Arndt, M.O. Baringer and M.R. Johnson, Eds.

Associate Eds. L.V.Alexander, H.J. Diamond, R.L. Fogt, J.M. Levy,
J. Richter-Menge, P.W.Thorne, L.A.Vincent, A.B.Watkins and K.M.Willett



(a) Yearly mean sea surface temperature anomalies (SSTA) in 2009 and (b) SSTA differences between 2009 and 2008. Anomalies are defined as departures from the 1971-2000 climatology. Refer to Chapter 3, Figure 3.1 for a more detailed description.

Special Supplement to the *Bulletin of the American Meteorological Society*
Vol. 91, No. 7, July 2010



f. Surface currents—R. Lumpkin, G. Goni, and K. Dohan

Near-surface currents are measured in situ by drogued satellite-tracked drifting buoys and by current meters on moored Autonomous Temperature Line Acquisition System (ATLAS) buoys.¹ During 2009, the drifter array ranged in size from a minimum of 778 drogued buoys to a maximum of 1149, with a median size of 937 drogued buoys (undrogued drifters continue to measure SST, but are subject to significant wind slippage; Niiler et al. 1987). The moored array included 38 buoys with current meters, all between 12°S and 21°N. These tropical moorings compose the Tropical Atmosphere Ocean (TAO; Pacific), Pilot Research Moored Array in the Tropical Atlantic (PIRATA; Atlantic) and Research Moored Array for African–Asian–Australian Monsoon Analysis and Prediction (RAMA; Indian) arrays.

Satellite-based estimates of ocean currents are produced using several methodologies, including the OSCAR (Ocean Surface Current Analyses–Real time) project, which uses satellite altimetry, winds, SST, and the Rio05 mean dynamic topography from the AVISO Ssalto/Duacs multimission altimeter gridded product (Rio and Hernandez 2004) to create one-degree resolution surface current maps averaged over the 0–30 m layer of the ocean (Bonjean and Lagerloef 2002). Anomalies are calculated with respect to the time period 1992–2007.

1) PACIFIC OCEAN

In the equatorial Pacific, the year began with a tapering off of the westward surface current anomalies at the end of 2008 (Fig. 3.15), bringing currents back to their climatological January values, although SST anomalies remained cold until April (Fig. 4.1). By February, eastward surface current anomalies were present on the equator from 160°E to 100°W. This El Niño pattern developed and intensified through May. In June–August, this pattern weakened in the central part of the basin, and near-climatological currents (or even westerly anomalies) were seen from the dateline to 120°E. The El Niño eastward anomalies began

¹ Drifter data is distributed by NOAA/AOML at <http://www.aoml.noaa.gov/phod/dac/gdp.html>. Moored data is distributed by NOAA/PMEL at <http://www.pmel.noaa.gov/tao>. OSCAR gridded currents are available at <http://www.oscar.noaa.gov/> and <http://podaac.jpl.nasa.gov/>. AVISO gridded altimetry is produced by SSALTO/DUACS and distributed with support from CNES, at <http://www.aviso.oceanobs.com/>. Analyses of altimetry-derived surface currents are available at <http://www.aoml.noaa.gov/phod/altimetry/cvar>.

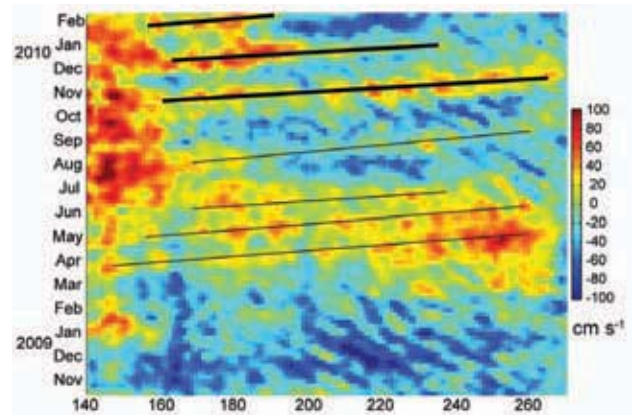


FIG. 3.15. Time-longitude plot of anomalous zonal equatorial currents (cm s^{-1}) from OSCAR. Black lines indicate eastward anomalies associated with propagating Kelvin waves.

redeveloping in August, in the form of eastward propagating Kelvin wave pulses that are concurrent with westerly wind anomalies (Fig. 3.15). Two major wave trains were generated at the start of October and December, resulting in strong eastward anomalies west of 140°E in October. In November through December, eastward anomalies dominated the entire equatorial band of the Pacific Ocean (Fig. 3.16).

Surface current anomalies in the equatorial Pacific typically lead SST anomalies by several months, with a magnitude that scales with the SST anomaly magnitude. Recovery to normal current conditions is also typically seen before SST returns to normal. Thus, current anomalies in this region are a valuable predictor of the evolution of SST anomalies and their related climate impacts. This leading nature can be

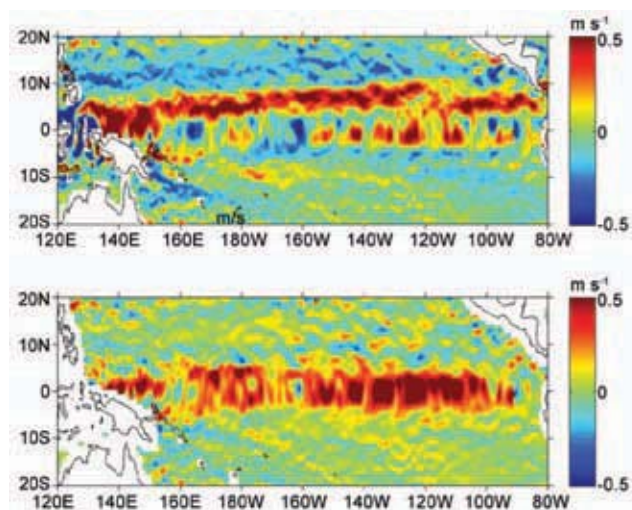


FIG 3.16. November 2009 zonal currents (top) and zonal current anomalies (bottom) in m s^{-1} , from OSCAR. Eastward anomalies exceeding 50 cm s^{-1} dominated most of the equatorial Pacific.

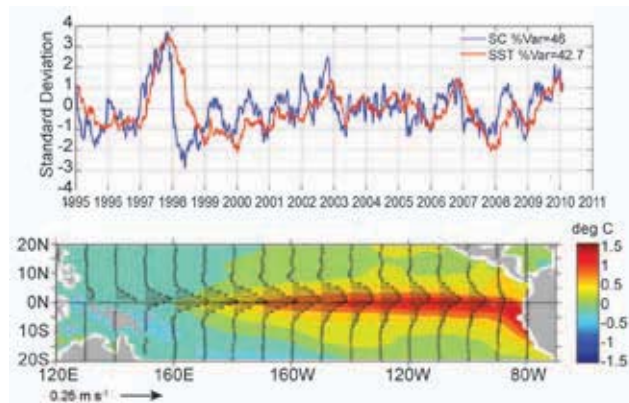


FIG 3.17. Principal empirical orthogonal functions (EOF) of surface current (SC) and of SST anomaly variations in the Tropical Pacific. (top) Amplitude time series of the EOFs normalized by their respective standard deviations. (bottom) Spatial structures of the EOFs.

seen clearly in the first principal EOF of surface current anomaly and separately of SST anomaly in the tropical Pacific basin (Fig. 3.17). By the end of 2009, the values of the normalized surface current and SST EOFs were reaching values approaching those of the 2002 El Niño, the strongest El Niño since the massive 1997–98 event.

The year ended with another strong wave pulse at the beginning of January 2010, together with a southward shift in westerly wind anomalies (Fig. 4.4), often associated with the onset of the termination of El Niño conditions (Lagerloef et al. 2003).

2) INDIAN OCEAN

The Agulhas Current in the southwestern Indian Ocean is the major western boundary current linking the Indian and South Atlantic basins. Its transport can be estimated on a monthly basis using a combination of altimetry and hydrographic climatology (see <http://www.aoml.noaa.gov/phod/altimetry/cvar/index.php>). In 2009, the baroclinic transport of the Agulhas decreased from a maximum seen in 2007, to $\sim 48 \text{ Sv}^2$, a value similar to those of the 1993–2000 period (Fig. 3.18, top). The generation of Agulhas rings, which carry Indian Ocean water into the Atlantic, decreased from the peak seen during 2007/08 (Fig. 3.18, bottom) to the more typical long-term average of ~ 5 rings yr^{-1} .

3) ATLANTIC OCEAN

In the tropical Atlantic, 2009, surface currents were close to climatology except during boreal spring.

Eastward anomalies of up to 50 cm s^{-1} occurred along the equatorial Atlantic in April through May, in response to weaker than normal Trade Winds that were also associated with anomalously cold SSTs in the northeastern Tropical Atlantic. This eastward anomaly pattern was disrupted in June–July, when westward anomalies developed east of 20°W in the Guinea Current region. By July, these currents had returned to normal climatological values.

Against the east coast of South America, the southward-flowing warm, salty Brazil Current meets the northward flowing cold, fresh Malvinas Current to create the Confluence Front.

Over the last 15 years, the location of this front has shifted to the south at a mean speed of nearly 1° latitude per decade (Goni et al. 2010, manuscript submitted to *Deep-Sea Res.*; Lumpkin and Garzoli 2010, manuscript submitted to *J. Geophys. Res.*). However, most of this shift occurred in the early part of the altimeter-derived time series; while it exhibits strong intraseasonal to seasonal fluctuations (Goni and Wainer 2001), its annual-averaged position has not changed significantly since 1998, and in 2009 it fluctuated between 37° and 39°S .

g. The meridional overturning circulation—M. O. Baringer, T. O. Kanzow, C. S. Meinen, S. A. Cunningham, D. Rayner, W. E. Johns, H. L. Bryden, J. J-M. Hirschi, L. M. Beal, and J. Marotzke

The meridional redistribution of mass and heat associated with the large-scale vertical circulation within the oceans is typically called the meridional overturning circulation (MOC). The most common definition of the strength of the MOC at any particular latitude is the maximum of the vertically integrated basinwide stream function, which changes as a function of latitude and time and is influenced by many physical systems embedded within it. There are several available estimates of the steady-state global mass, fresh water, and heat transport based on the best available hydrographic data (Talley 2008; Lumpkin and Speer 2007; Ganachaud and Wunsch 2003), as well as a few local estimates of the MOC from one-time full water column hydrographic sections and western boundary arrays (e.g., McDonagh et al. 2008; Kanzow et al. 2008); however, true time-series observations of basinwide MOC transports are logistically very challenging to collect.

Substantial progress has been made on developing a coordinated observing system to measure the MOC through the international conference called OceanObs09 held September, 2009. The conference resulted in numerous community white papers and

² Sv is a Sverdrup or $10^6 \text{ m}^3 \text{ s}^{-1}$, a unit commonly used for ocean volume transports.